医薬品研究
Pharm. Regul. Sci.
37(7)448～456(2006)

——資　　料——

平成16年度「日本薬局方の試験法に関する研究」研究報告

局方組換えタンパク質性医薬品の糖鎖試験法に関する研究**
—LC/MS^{n}を用いた糖鎖プロファイリング—

川崎　ナナ，伊藤さつき，橋井　則貴，日向　昌司，川西　徹*

1．はじめに

日本薬局方第14改正に組換え医薬品として初めてヒトインスリンが収載され，今後多くの組換え医薬品が新規収載されることが予想されている．現在までに承認された組換え医薬品や開発段階にある組換え医薬品の多くが糖タンパク質であることを考えると，新規収載品の多くが糖タンパク質性医薬品となることは確実であろう．糖タンパク質は同一ポリペプチド鎖に様々な糖鎖が結合した複数の分子からなる不均一な集合体で，その不均一性の変化は，活性，体内動態，安定性，溶解性，及び安全性に直接影響を与えることが多くの研究により明らかにされている[1]．しかも糖鎖付加は，人為的に制御することが困難である上，製造方法に依存して変動することから，糖タンパク質関連医薬品の品質評価において，糖鎖部分の恒常性を確認することが重要である．

第15改正にSDSポリアクリルアミドゲル電気泳動法，タンパク質定量法，等電点電気泳動法，アミノ酸分析法，キャピラリー電気泳動法，及びペプチドマップ法が参考情報として収載される．しかし，糖タンパク質の糖鎖に関する試験法の収載は，検討されていない．それは，糖鎖の構造が複雑で不均一性が高く，解析が容易ではないことに起因している．現在のところ，糖鎖分析法として，単糖組成分析や，各種HPLC及び電気泳動法を用いた糖鎖プロファイリングなどが検討されているが，国際的にも定まった試験法がないのが現状である．製造方法変更に伴うバイオ医薬品の同等性/同質性評価や，バイオ後発品の同等性/同質性評価において，糖鎖部分の評価が重要視されている昨今，糖鎖試験法の整備は急務である．

我々はこれまで，液体クロマトグラフィー/質量分析法（LC/MS）を用いた独自の糖鎖プロファイリング法を開発し，様々な糖タンパク質の糖鎖構造解析に応用してきた[2~4]．この方法は，グラファイトカーボンカラム（GCC）を用いて多様な糖鎖を分離しながら，直接エレクトロスプレーイオン化（ESI）MS及びタンデムMS（MS/MS）で分子量測定と糖鎖配列解析を行うもので，1回の分析で，糖鎖の不均一性や個々の糖鎖の構造情報を得ることができる．本研究では，短時間でより多くの糖鎖を識別し，構造情報を得ることを目的として，LC/MSを用いた糖鎖プロファイリング法の改良を行った．すなわち，ポジティブ及びネガティブイオンモードにおける連続多段階MS（MS^n）の利用，並びにLC/MSに適した試料調製法として，従来の糖鎖の還元化に加えて，国内での汎用性の高いピリジルアミノ（PA）化の利用を検討した．更に，糖タンパク質のモデルとして遺伝子組換え型ヒト絨毛性性腺刺激ホルモン（rhCG），及び糖鎖構造を改変した組換え型ヒトフォリスタチンを用い，糖鎖試験法としての可能性を検証した．

2．研究方法

【試薬・材料】

還元糖鎖はLudger社及びGLYCO社より購入した．PA化糖鎖はコスモ・バイオ社より購入した．

* 国立医薬品食品衛生研究所生物薬品部　東京都世田谷区上用賀1-18-1（〒158-8501）
** 本研究は日本公定書協会の「日本薬局方の試験法に関する研究」により行ったものである．

遺伝子組換え型rhCGはシグマ社より購入した．フォリスタチンは，*N*-アセチルグルコサミン（GlcNAc）転移酵素-III（GnT-III）遺伝子を導入したCHO細胞で発現させ，硫酸化セルロファインカラム及びC4カラムを用いたHPLCで精製した．

【rhCG糖鎖の調製】

rhCG（200 μg）を8 Mグアニジン塩酸塩，5 mM EDTAを含む0.5 M Tris-HCl，pH 8.6（270 μL）に溶解し，2-メルカプトエタノール2 μLを加え，室温で2時間放置した．モノヨード酢酸ナトリウム5.7 mgを試料溶解溶液45 μLに溶かして試料溶液に加え，遮光下，室温にて2時間放置した．PD-10カラム（Amersham Bioscience）を用いて脱試薬し，得られた試料溶液を凍結乾燥した．還元カルボキシメチル化rhCG（100 μg）を95 μLの0.1 Mリン酸緩衝液（pH 7.2）に溶解し，5 μLの*N*-グリコシダーゼF（PNGaseF）と37℃で18時間反応させて糖鎖を切り出した．終濃度が70%になるように冷エタノールを加えてタンパク質を沈殿させ，上清をSpeedVacで減圧乾固した．糖鎖を50 μLの水に溶解し，0.5 M $NaBH_4$（50 μL）と反応させて糖アルコールとした．カーボンカートリッジENVI-Carb（Supelco）を用いて脱塩し，減圧乾固後，50 μLの水に溶解して試料溶液とした．

【フォリスタチン糖鎖の調製】

精製したフォリスタチン（200 μg）を還元カルボキシメチル化し，0.1 Mリン酸緩衝液（pH 7.2）中でPNGase F（5単位）と37℃で16時間反応させて糖鎖を切り出した．70%冷エタノールを加えてタンパク質を沈殿させ，上清をSpeedVacで減圧乾固した．糖鎖に20 μLのカップリング試薬（12.8 M AP－酢酸溶液）を加えて90℃で60分間反応させた．反応液に20 μLの還元試薬（3.3 Mボランジメチルアミン複合体－酢酸溶液）を加えて80℃で60分加熱して還元した．更に，反応液にトリエチルアミン－メタノール（40 μL）及びトルエン（50 μL）を加えた後，窒素気流下減圧乾固した（60℃，15分間）．過剰の未反応試薬は残渣にメタノール（20 μL）及びトルエン（40 μL）を加えた後，窒素気流下減圧除去した（60℃，10分間）．更に50 μLのトルエンを残渣に加えた後，窒素気流下減圧乾固した（50℃，10分間）．PA糖鎖を5 mM酢酸アンモニウム溶液に溶解し，ENVI-Carbを用いて脱塩した後，50 μLの5 mM酢酸アンモニウム溶液に溶かして試料溶液とした．

【LC/MSⁿ】

HPLC：

装置：Paradigm MS4（Michrom BioResource社）

カラム：Hypercarb（Thermo Electron社，0.2又は0.1×150 mm，5 μ）

溶離液A：2%アセトニトリルを含む5 mM酢酸アンモニウム水溶液（pH 9.6）

溶離液B：80%アセトニトリルを含む5 mM酢酸アンモニウム水溶液（pH 9.6）

グラジエントプログラム：

B液：5～40%（0～60分）（還元化糖鎖の分離）

：10～45%（0～60分）（PA化糖鎖の分離）

流速：2 μL/min

MSⁿ：

装置：LTQ-FT（Thermo Electron社）

イオン源：nanoESI（AMR社）

キャピラリー温度：200℃

キャピラリー電圧：1.8 kV

スキャン範囲（m/z）：450～2,000

衝突エネルギー：35%

3．実験結果

3.1 糖鎖プロファイリング法の改良

還元糖鎖のアノマーは逆相系HPLCによって互いに分離されるので，LC/MSを行うにあたって，あらかじめ還元末端を誘導体化しておく必要がある．そこで，標準糖鎖（Fig. 1A, B, C及びD）を$NaBH_4$で還元して糖アルコール（各0.5 pmol）とし，これらをモデル糖鎖としてLC/MSⁿを用いた糖鎖プロファイリングの改良を検討した．分離用カラムとして内径0.1 mmのグラファイトカーボンカラム，及び質量分析装置としてナノESIを接続したイオントラップ型MS-イオンサイクロトロン共鳴質量分析（ITMS-FT ICRMS）装置を用い，ポジティブイオンモードにおけるFT ICRMSを用いたフルMS¹スキャン及びITMSを用いたデータ依存的MS²⁻⁴スキャン，並びにネガティブイオンモードにおけるFT ICRMSを用いたフルMS¹スキャン及びITMSを用いたデータ依存的MS²⁻⁴スキャンを1サイクルとしてLC/MSⁿを行った．なお，デ

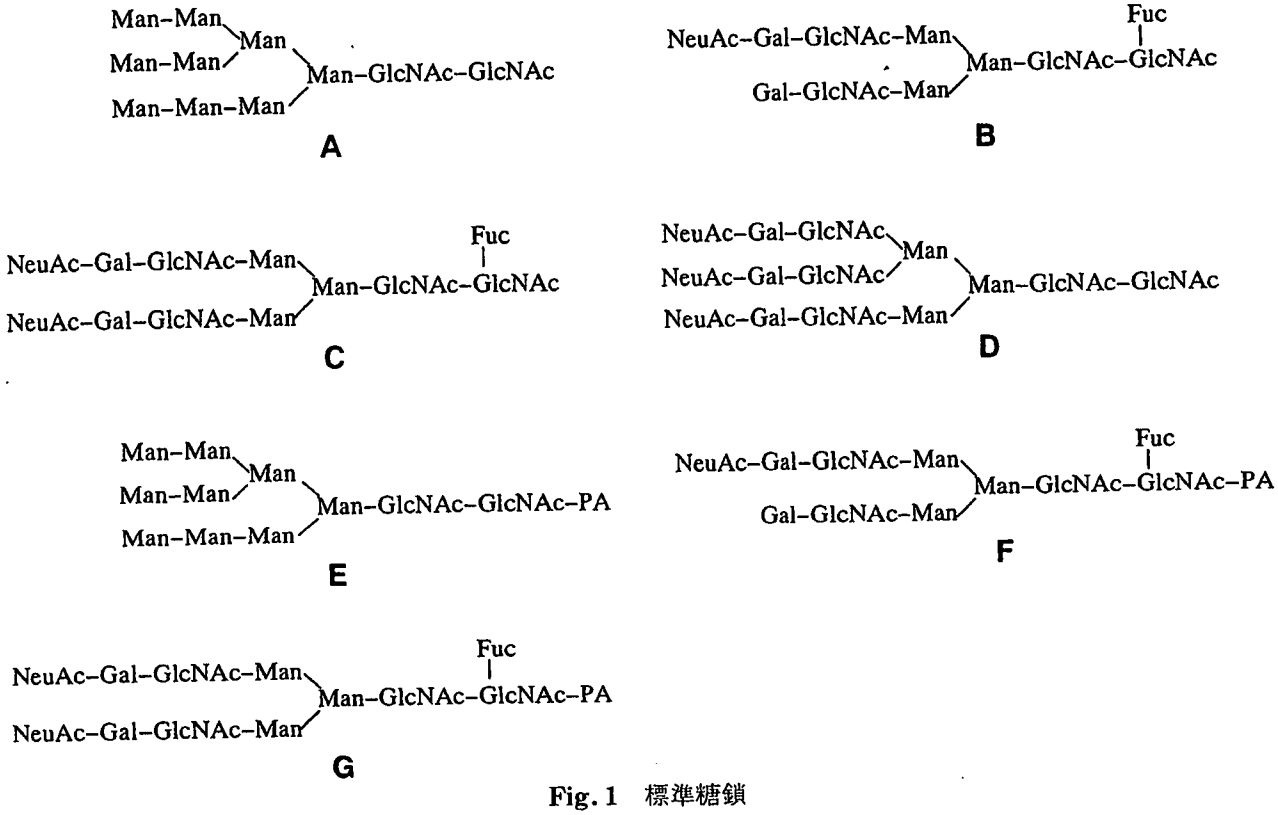

Fig. 1 標準糖鎖

ータ依存的 MS$^{2-4}$ は，その前のスキャンにおいて最も強度の高い前駆イオンに対して行った．

Fig. 2A 及び B は，ポジティブ及びネガティブイオンモードにおいて FT ICRMS を用いたフル MS^1 スキャンによって得られたトータルイオンクロマトグラム（TIC）である．検出された 5 つのピーク（ピーク 1～5）は，MS^1 で得られた分子量と MS$^{2-4}$ で得られたプロダクトイオンから，Fig. 2 中に示すように，マンノース 9 分子からなる糖鎖（Man9）(Fig. 1A)，*N*-アセチルノイラミン酸（NeuAc）が 1 個結合したフコシル 2 本鎖糖鎖（Fig. 1B），NeuAc が 2 分子結合したフコシル 2 本鎖糖鎖（Fig. 1C），及び 2 種類のトリシアロ 3 本鎖糖鎖（Fig. 1D）と帰属された．一例として，Fig. 3A，B，及び C に，ピーク 2 のポジティブ及びネガティブイオンモードにおける FT ICRMS を用いたフル MS^1 スペクトル，及び m/z 1040.89 のイオンを前駆イオンとした MS^2 スペクトルを示す．MS^1 で得られた分子量，及び MS^2 スペクトルに観測された一連の B イオンシリーズ，及び Y イオンシリーズは，モノシアロフコシル 2 本鎖糖鎖（Fig. 1B）の構造と矛盾がない．

ポジティブイオンモードで強く検出される Man9 は，ネガティブイオンモードでは小さなピークとして検出された．このことは，中性糖鎖はポジティブイオンモードでの測定が適していることを示唆している．酸性糖鎖であるトリシアロ 3 本鎖糖鎖は，ポジティブ及びネガティブ両イオンモードで検出されたが，糖鎖にはより酸性度の高い硫酸化糖鎖やポリシアロ糖鎖などが存在することから，ネガティブイオンモードでの検出が必要と考えられる．以上のように，ポジティブ及びネガティブイオンモードにおける MS$^{1-4}$ を 1 サイクルとして連続分析することによって，多様な構造を含む糖タンパク質の糖鎖を一度に解析することが可能となった．

3.2 rhCG 糖鎖プロファイリングへの応用

hCG は局方収載の代表的糖タンパク質で，α サブユニット，及び β サブユニットから構成されている[5]．α サブユニットは 92 アミノ酸残基からなり，Asn52 と 78 に *N* 結合型糖鎖が結合している．β サブユニットは 145 アミノ酸残基からなり，Asn13 と 30 に *N* 結合型糖鎖，並びに Ser121，127，132，

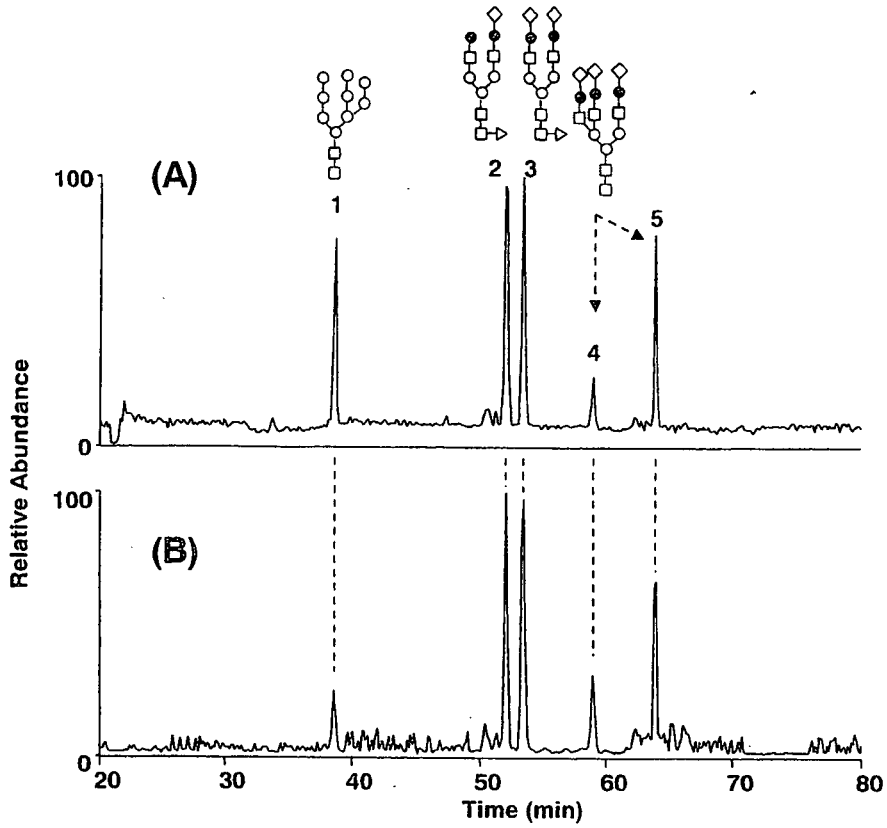

Fig. 2　標準糖鎖（Fig. 1A-D）のLC/MS^{1}によって得られたTICと主なピークの糖鎖構造
(A) ポジティブイオンモード　(B) ネガティブイオンモード
◇, NeuAc; ○, Man; ●, Gal; □, GlcNAc; △, Fuc

及び138に*O*結合型糖鎖が付加している．LC/MS^{n}を用いた糖鎖プロファイリング法を，rhCGの*N*結合型糖鎖の解析に応用した．

糖鎖の切り出しを完全に行うため，rhCGを還元カルボキシメチル化した後，PNGaseFを作用させた．切り出した糖鎖は，$NaBH_4$を用いて還元した．Fig. 4A及びBは，ポジティブ及びネガティブイオンモードにおけるフルMS^{1}スキャンによって得られたrhCG（6 μg）の糖鎖プロファイルである．各ピークの糖鎖構造は，MS^{1}によって測定された分子量及びMS^{2}によって検出されたプロダクトイオンから推定した．その結果，Fig. 4中に示すように，rhCGの主な糖鎖の構造はシアル酸が結合した混成型及び複合型2本鎖で，一部3本鎖糖鎖が含まれることが確認された．このように改良型糖鎖プロファイリング法は，糖タンパク質糖鎖の分布と個々の糖鎖の構造の確認に利用できることが示された．

3.3　PA化標準糖鎖を用いた糖鎖プロファイリング

PA化法は長谷らによって開発された糖鎖誘導体法で，PA化法と2(3)種類のHPLCを組み合わせた糖鎖解析法は，2(3)次元糖鎖マッピングとしてよく知られている[6,7]．PA化された糖鎖が標準物質として入手可能であることや，解析のためのプロトコールが整備されていることから，PA化とHPLCの組み合わせは，国内で最も利用されている糖鎖構造解析法・試験法の一つとなっている．PA化は汎用性が高い糖鎖誘導体化法であることから，つぎに，PA化糖鎖のLC/MS^{n}を検討した．

Fig. 5は，LC/MS^{1}によって得られたPA化標準糖鎖（Figs. 1E, F, 及びG, 各5 pmol）のベースピーククロマトグラムである．各ピークの糖鎖の構造は，分子量とデータ依存的に測定したMS^{2}スペクトルから帰属した．Fig. 6に一例としてピーク3

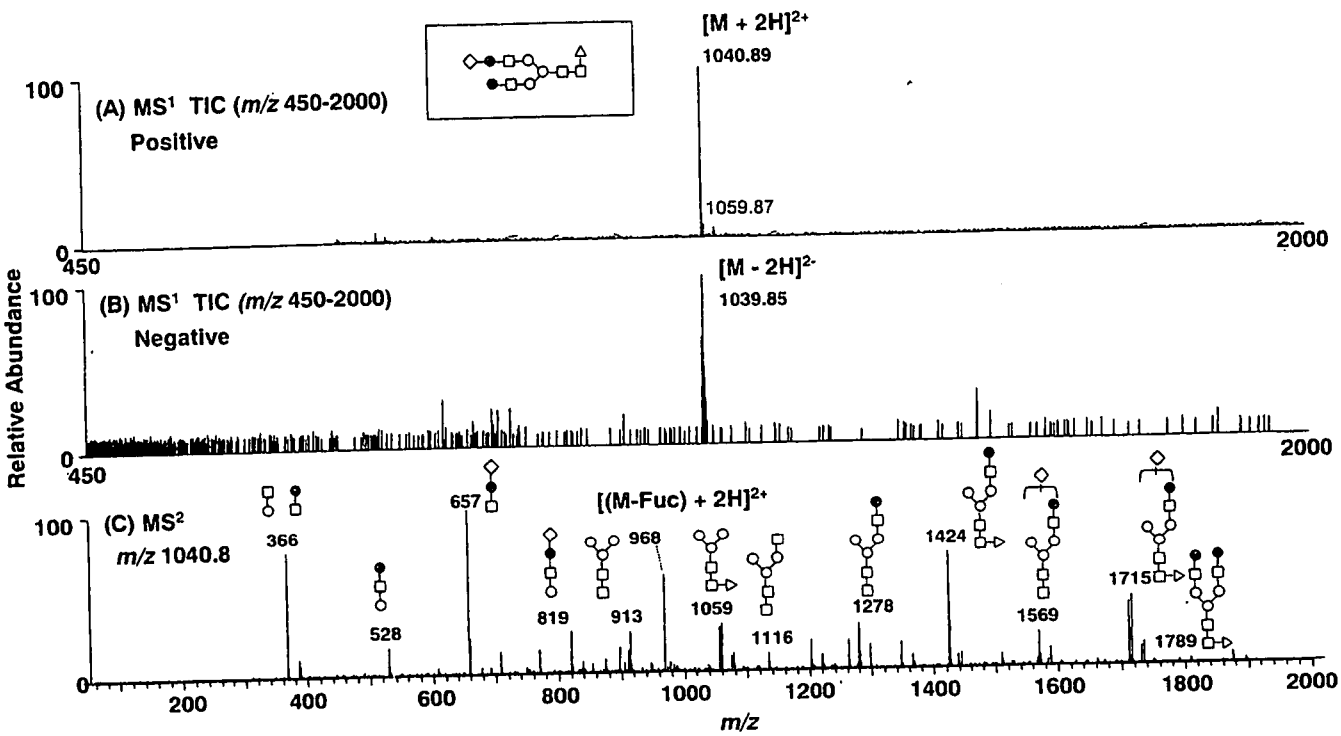

Fig. 3 Fig. 2 中のピーク 2 の代表的マススペクトル
(A) フル MS^1, ポジティブイオンモード (B) フル MS^1, ネガティブイオンモード (C) MS^2, 前駆イオン：m/z 1040.8, ポジティブイオンモード

の MS^2 スペクトルを示す．還元化糖鎖と同様に，B イオンシリーズ及び Y イオンシリーズが検出され，糖鎖の配列に関する情報が得られていることが確認された．このように，PA 化糖鎖の LC/MS^n は，$NaBH_4$ 還元化糖鎖と同様な構造情報が得られることから，糖タンパク質の糖鎖解析及び確認に適していることが示唆された．

3.4 糖鎖改変タンパク質の糖鎖プロファイリングへの応用

LC/MS^n を，今後バイオ医薬品として開発される可能性が高い糖鎖改変型タンパク質の糖鎖試験に応用することを目的として，糖鎖改変遺伝子組換え型ヒトフォリスタチンの糖鎖プロファイリングを行った．フォリスタチンは，細胞の分化・増殖を促す因子であるアクチビンと複合体を形成することによって，アクチビンの受容体への結合を阻害し，アクチビンの様々な作用，すなわち，赤芽球系細胞の分化誘導，神経細胞生存維持，及び生殖細胞の分化誘導作用等を中和する糖タンパク質である[8]．先に我々は，フォリスタチンの Asn95 及び Asn259 に N 結合型糖鎖が部分的に結合していること，及びそれらの糖鎖構造を明らかにしている[9]．本研究では，N 結合型糖鎖のトリマンノシルコアのマンノースに bisecting と呼ばれる GlcNAc を β1-4 結合させる GnT-III の遺伝子を導入した CHO 細胞でフォリスタチンを発現させ，PA 標識と LC/MS^n を用いた糖鎖プロファイリングが，糖鎖構造の変化を明らかにすることができるかを調べた．

Fig. 7 は PA 化した糖鎖改変フォリスタチン由来糖鎖の LC/MS^1 によって得られたベースピーククロマトグラムである．MS^1 によって得られた分子量及び MS^2 によって得られた糖鎖配列情報から，糖鎖改変フォリスタチンの主な糖鎖構造は，Fig. 7 に示すように推定された．主なピークの糖鎖構造は，先に我々が報告した CHO 細胞由来組換え非改変型フォリスタチンの糖鎖の構造に一致していたが，改変型フォリスタチンには非改変型フォリスタチンには認められなかった糖鎖（ピーク a）が認められた．ピーク a は，分子量からモノガラクトシル 2 本鎖糖鎖に GlcNAc が 1 分子付加した糖鎖と推定され

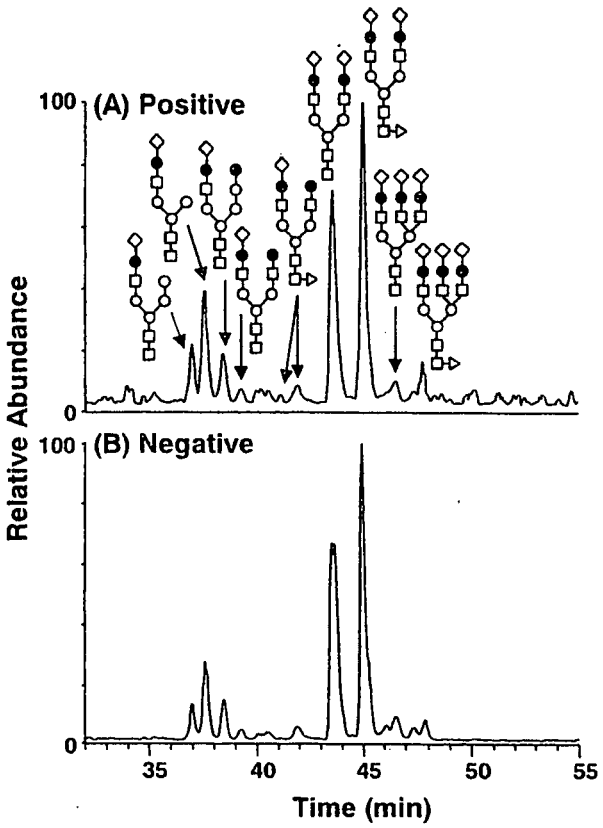

Fig. 4　rhCG由来還元化N結合型糖鎖のLC/MS^{1}によって得られたトータルイオンクロマトグラム
(A) ポジティブイオンモード　(B) ネガティブイオンモード

たが，分子量からは，3本鎖糖鎖か，bisecting GlcNAcが結合した2本鎖糖鎖であるかを決定できなかった．そこで，MS^{2,3}スペクトルを精査したところ，MS^{3}スペクトルのm/z 869.3及び1015.3にbisecting GlcNAcに特徴的なプロダクトイオンが検出されていることが確認された（Fig. 8）．これらのイオンから，この糖鎖は，GnT-III遺伝子導入によって出現したbisecting GlcNAcが結合した2本鎖糖鎖であることが明らかになった．このように，LC/MS^{n}を用いた糖鎖プロファイリングは，糖鎖の僅かな変化を明らかにできること，また，配列が異なる異性体を識別できることから，糖鎖改変型タンパク質の糖鎖確認に応用可能であることが示された．

4．考　察

糖鎖部分の恒常性を確保するため，多くの糖タンパク質性医薬品の品質試験において，遊離糖鎖のプロファイリングが設定されている．これまでは，2-アミノピリジンや2-アミノベンザミドによる糖鎖の標識とHPLCの組み合わせや，HPAEC-PADが糖鎖プロファイリングに利用されてきた．これらの方法は定量性には優れているが，溶出位置が接近している糖鎖を識別できないなどの問題があることから，定性的にもすぐれた試験法の開発が望まれている．

我々は，豊富な構造情報が得られるLC/MSを取り入れた独自の糖鎖プロファイリング法を開発し，エリスロポエチン[2]，肝細胞増殖因子[3]，甲状腺刺激ホルモン，トロンボモジュリン[4]等の構造特性解析に応用してきた．この方法の試験法への応用を目的として，本研究ではまず，$NaBH_4$で還元した標準的なN結合型糖鎖を用いて，精密分子量測定，ポジティブ及びネガティブイオンモードにおける連続MS^{n}を取り入れた改良型糖鎖プロファイリング法を検討し，一度の分析で中性糖鎖及び酸性糖鎖を迅速・簡便に解析することに成功した．また，国内での汎用性が高く，様々な標準糖鎖が市販されているPA化糖鎖を使って糖鎖プロファイリングを行うことを検討し，還元化糖鎖と同様に構造解析できることを確認した．更に，LC/MS^{n}を用いた糖鎖プロファイリング法は，代表的糖タンパク質のrhCGや，糖鎖改変によって僅かに変化した糖鎖のプロファイリングにも利用できることを確認した．

本研究を通してLC/MS^{n}を用いた糖鎖プロファイリングは，LC上の溶出位置の違いだけでなく，分子量の違い，更には糖鎖配列の違いから糖鎖を識別できることが確認された．以上のことから，LC/MS^{n}を用いた糖鎖プロファイリングは，糖タンパク質性医薬品の糖鎖試験法として応用可能であることが示唆された．また，本分析法は，糖鎖の識別だけでなく，構造解析にも有用であることから，新規糖タンパク質性医薬品の特性解析・品質評価，糖鎖改変タンパク質の糖鎖解析，製造方法変更時における同等性/同質性評価，並びにバイオ後発医薬品の評価等にも応用できると思われる．

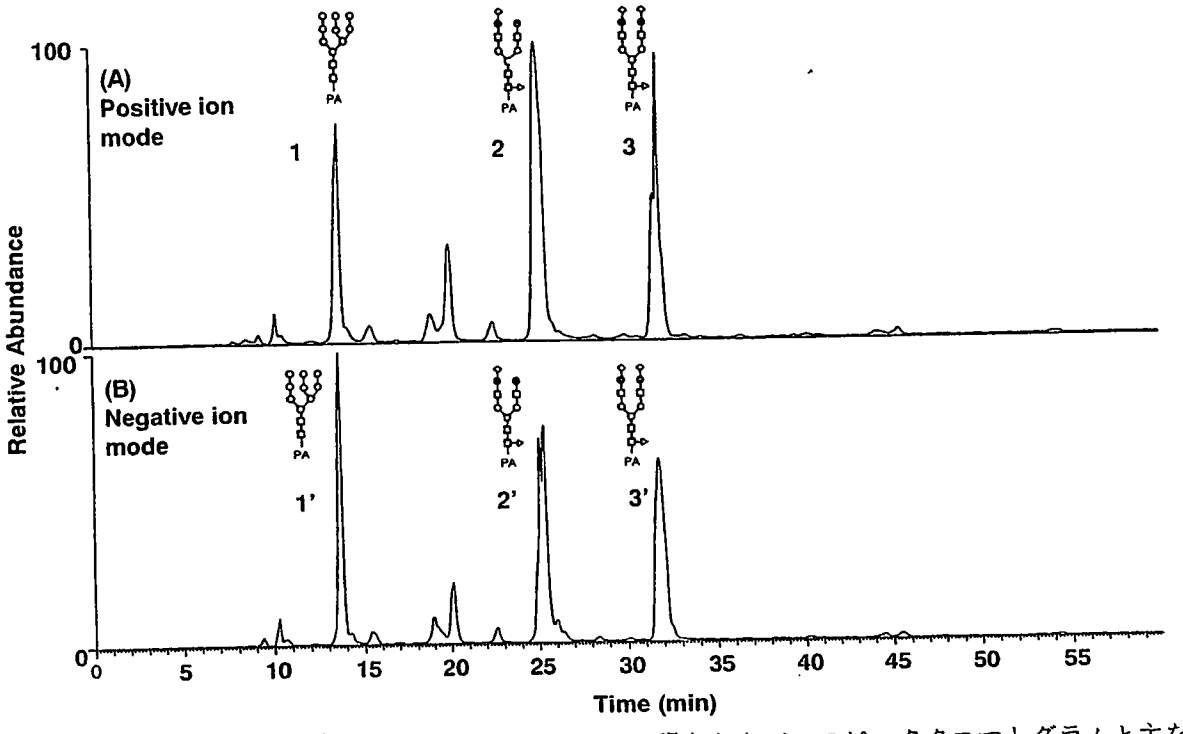

Fig. 5 標準 PA 糖鎖（Fig. 1E-G）の LC/MS^1 によって得られたベースピーククロマトグラムと主なピークの糖鎖構造
（A）ポジティブイオンモード （B）ネガティブイオンモード

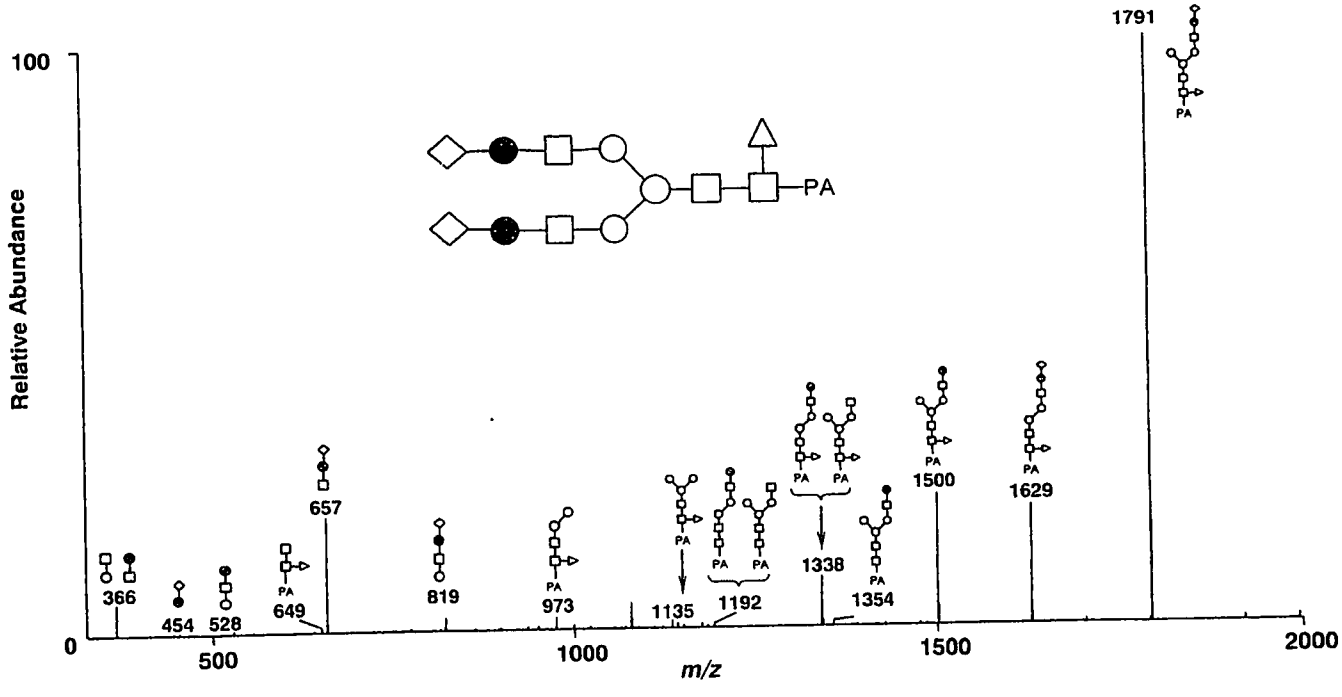

Fig. 6 Fig. 5 中のピーク 3 の代表的 MS^2 スペクトル
前駆イオン：m/z 1225，ポジティブイオンモード

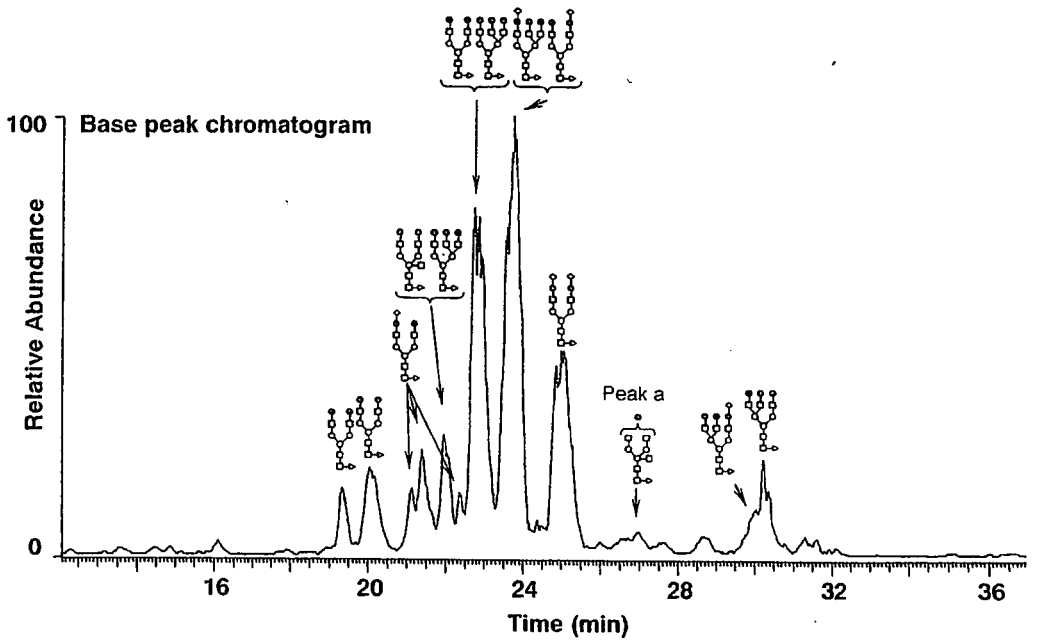

Fig. 7　GnT-III 遺伝子導入 CHO 細胞で発現させた糖鎖改変型フォリスタチン由来 PA 化糖鎖の LC/MS^1 によって得られたベースピーククロマトグラム

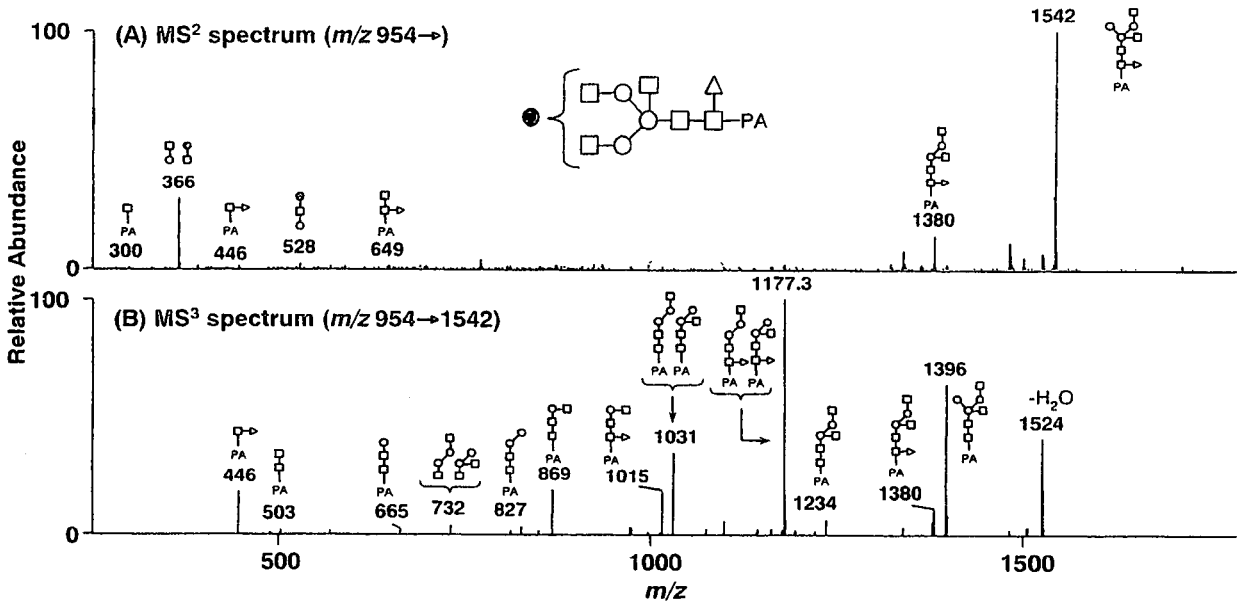

Fig. 8　Fig. 7 中のピーク a の代表的 MS^{2,3} スペクトル
(A) MS^2 スペクトル　前駆イオン：m/z 954, ポジティブイオンモード
(B) MS^3 スペクトル　前駆イオン：m/z 1542, ポジティブイオンモード

文　献

1) Varki, A.: *Glycobiology*, **3**, 97-130 (1993).
2) Kawasaki, N., Ohta, M., Hyuga, S., Hyuga, M., Hayakawa, T.: *Anal. Biochem.*, **285**, 82-91 (2000).
3) Kawasaki, N., Itoh, S., Ohta, M., Hayakawa, T.: *Anal. Biochem.*, **316**, 15-22 (2003).
4) Itoh, S., Kawasaki, N., Ohta, M., Hyuga, M., Hyuga, S., Hayakawa, T.: *J. Chromatogr, A*, **978**, 141-152 (2002).
5) Kobata, A.: *J. Cell Biochem.*, **37**, 79-90 (1988).
6) Hase, S., Ibuki, T., Ikenaka, T.: *J. Biochem.*, **95**, 197-203 (1984).
7) Tomiya, N., Kurono, M., Ishihara, H., Tejima, S., Endo, S., Arata, Y., Takahashi, N.: *Anal. Biochem.*, **163**, 489-499 (1987).
8) Nakamura, T., Takio, K., Eto, Y., Shidai, H., Titani, K., Sugino, H.: *Science*, **247**, 836-838 (1990).
9) Hyuga, M., Itoh, S., Kawasaki, N., Ohta, M., Ishii, A., Hyuga, S., Hayakawa, T.: *Biologicals*, **32**, 70-77 (2004).

Available online at www.sciencedirect.com
SCIENCE DIRECT
Analytical Biochemistry 348 (2006) 259–268
ANALYTICAL BIOCHEMISTRY
www.elsevier.com/locate/yabio

Site-specific N-glycosylation analysis of human plasma ceruloplasmin using liquid chromatography with electrospray ionization tandem mass spectrometry

Akira Harazono *, Nana Kawasaki, Satsuki Itoh, Noritaka Hashii, Akiko Ishii-Watabe, Toru Kawanishi, Takao Hayakawa

National Institute of Health Sciences, Division of Biological Chemistry and Biologicals, 1-18-1 Kami-yoga, Setagaya-Ku, Tokyo 158-8501, Japan

Received 8 June 2005
Available online 10 November 2005

Abstract

Ceruloplasmin has ferroxidase activity and plays an essential role in iron metabolism. In this study, a site-specific glycosylation analysis of human ceruloplasmin (CP) was carried out using reversed-phase high-performance liquid chromatography with electrospray ionization tandem mass spectrometry (LC-ESI-MS/MS). A tryptic digest of carboxymethylated CP was subjected to LC-ESI-MS/MS. Product ion spectra acquired data-dependently were used for both distinction of the glycopeptides from the peptides using the carbohydrate B-ions, such as *m/z* 204 (HexNAc) and *m/z* 366 (HexHexNAc), and identification of the peptide moiety of the glycopeptide based on the presence of the b- and y-series ions derived from the peptide. Oligosaccharide composition was deduced from the molecular weight calculated from the observed mass of the glycopeptide and theoretical mass of the peptide. Of the seven potential N-glycosylation sites, four (Asn119, Asn339, Asn378, and Asn743) were occupied by a sialylated biantennary or triantennary oligosaccharide with fucose residues (0, 1, or 2). A small amount of sialylated tetraantennary oligosaccharide was detected. Exoglycosidase digestion suggested that fucose residues were linked to reducing end GlcNAc in biantennary oligosaccharides and to reducing end and/or α1–3 to outer arms GlcNAc in triantennary oligosaccharides and that roughly one of the antennas in triantennary oligosaccharides was α2–3 sialylated and occasionally α1–3 fucosylated at GlcNAc.

Keywords: Ceruloplasmin; Glycopeptide; Liquid chromatography-electrospray tandem mass spectrometry; Product ion spectrum; Exoglycosidase digestion

Ceruloplasmin (CP)[1] is a blue copper serum glycoprotein synthesized in the liver. CP has ferroxidase activity and plays an essential role in iron metabolism [1–4]. The primary structure of human CP has been determined by amino acid sequencing, and it is composed of a single polypeptide chain of 1046 amino acid residues [5]. The amino acid sequence was confirmed from complete cDNA sequence [6]. The major oligosaccharides in human CP were reported to be sialylated bi- and triantennary structures with or without a fucose residue [7,8]. Although four N-glycosylation sites (Asn119, Asn339, Asn378, and Asn743) were identified among seven potential sites [9], the heterogeneity of oligosaccharides was still unknown at each glycosylation site. CP is an acute phase reactant, and the serum concentration increases during inflammation, infection, and trauma [10]. It is known that the patterns of glycosylation are changed by inflammatory cytokines [11]. Several studies have reported that CP is a good diagnostic marker of solid malignant tumors [12,13] and that the CP glycoform might

* Corresponding author. Fax: +81 3 3700 9084.
E-mail address: harazono@nihs.go.jp (A. Harazono).

[1] *Abbreviations used:* CP, ceruloplasmin; LC-ESI-MS, liquid chromatography with electrospray ionization mass spectrometry; Hex, hexose; HexNAc, *N*-acetylhexosamine; LC-ESI-MS/MS, liquid chromatography with electrospray ionization tandem mass spectrometry; EDTA, ethylenediaminetetraacetic acid; TFA, trifluoroacetic acid; Q-TOF, quadrupole time-of-flight; TIC, total ion chromatogram; NeuAc, *N*-acetylneuraminic acid; GlcNAc, *N*-acetylglucosamine; Fuc, fucose.

0003-2697/$ - see front matter © 2005 Elsevier Inc. All rights reserved.
doi:10.1016/j.ab.2005.10.036

be a valuable supplement [12]. Thus, it is important to conduct a site-specific glycosylation analysis of normal human CP.

One of the most effective techniques for determining the site-specific carbohydrate heterogeneity of glycoproteins is the mass spectrometric peptide mapping of proteolytic fragments of glycoproteins by liquid chromatography with electrospray ionization mass spectrometry (LC-ESI-MS) [14–19]. The specific detection of glycopeptides in a complex peptide mixture is generally achieved by monitoring specific carbohydrate fragment ions such as *m/z* 204 (HexNAc) and *m/z* 366 (HexHexNAc) produced by cone voltage fragmentation or by precursor ion scanning [15–19]. Because product ion spectra of glycopeptides show high abundant carbohydrate fragment ions and low abundant b- and y-series fragment ions derived from the peptide backbone [20,21], product ion spectra acquired data-dependently in liquid chromatography with electrospray ionization tandem mass spectrometry (LC-ESI-MS/MS) can be used for both the selection from the peptides and the identification of the glycopeptides [22]. MS in combination with specific exoglycosidase digestions allows us to obtain the site-specific information on anomericity and linkage of glycans [23]. In the current study, we conducted a site-specific glycosylation analysis of human CP and successfully determined glycosylation status and glycosylation profile at each N-glycosylation site.

Materials and methods

Materials

Acetonitrile, formic acid, and guanidine hydrochloride were purchased from Wako Pure Chemicals Industries (Osaka, Japan). Purified human CP was purchased from Calbiochem (San Diego, CA, USA). Modified trypsin was purchased from Promega (Madison, WI, USA). α2–3 Neuraminidase (EC 3.2.1.18) of *Macrobdella decora*, a recombinant form, and α1–3,4 fucosidase (EC 3.2.1.51) from *Xanthomonas* sp. were purchased from Calbiochem. α2–3,6,8,9 Neuraminidase (EC 3.2.1.18) of *Arthrobacter ureafaciens*, a recombinant form, and β1–4 galactosidase (EC 3.2.1.23) were purchased from Sigma Chemical (St. Louis, MO, USA). The water used was obtained from a Milli-Q water system (Millipore, Bedford, MA, USA). All other reagents were of the highest quality available.

Reduction and S-carboxymethylation of CP

CP (100 μg) was dissolved in 270 μl of 0.5 M Tris–HCl buffer (pH 8.5) that contained 8 M guanidine hydrochloride and 5 mM ethylenediaminetetraacetic acid (EDTA). After the addition of 2 μl of 2-mercaptoethanol, the mixture was incubated for 2 h at 40 °C. Then 5.67 mg of monoiodoacetic acid was added, and the resulting mixture was incubated for 2 h at 40 °C in the dark. The reaction mixture was applied to a PD-10 column (Amersham Biosciences, Uppsala, Sweden) to remove the reagents, and the eluate was lyophilized.

Trypsin digestion of CP

Reduced and carboxymethylated CP was redissolved in 100 μl of 0.1 M Tris–HCl buffer (pH 8.0). An aliquot of 1 μl of trypsin prepared as 1 μg/μl was added to 50 μl of CP solution (1:50, w/w), and the mixture was incubated for 16 h at 37 °C. The enzyme digestion was stopped by storing at −20 °C before analysis.

HPLC of tryptic digest of CP

Tryptic digests (0.2 and 0.4 μg) of human CP were analyzed by LC-ESI-MS/MS to identify the peptides and glycopeptides, respectively. HPLC was performed on a Paradigm MS 4 (Michrome BioResources, Auburn, CA, USA) equipped with a Magic C18 column (0.2 μ, 50 mm, Michrome BioResources). The eluents consisted of water containing 2% (v/v) acetonitrile and 0.1% (v/v) formic acid (pump A) and 90% acetonitrile and 0.1% formic acid (pump B). Trypsin-digested samples were loaded onto a microtrap (peptide captrap, Michrom BioResources). After a wash with 15 μl H_2O/CH_3CN (98:2) with 0.1% trifluoroacetic acid (TFA), the trapping column was switched into line with the column. Samples were eluted with 5% of B for 10 min, followed by a linear gradient from 5 to 65% of B in 60 min at a flow rate of 2 μl/min.

ESI-Q-TOF-MS/MS

Mass spectrometric analyses were performed using a quadrupole time-of-flight (Q-TOF) mass spectrometer (QSTAR Pulsar, MDS Sciex, Toronto, Canada) equipped with a nano-electrospray ion source. The mass spectrometer was operated in the positive ion mode. The nanospray voltage was set at 2500 V. Mass spectra were acquired at *m/z* 400–2000 or *m/z* 1000–2000 for MS analysis and at *m/z* 100–2000 for MS/MS analysis. After every regular MS acquisition, two MS/MS acquisitions against top two of the multiply charged molecular ions were performed (data-dependent acquisition). The precursor ions with the same *m/z* as acquired previously were excluded for 120 s. The collision energy was varied between 30 and 80 eV depending on the size and charge of the molecular ion. Accumulation times for the spectra were 1.0 and 2.0 s for MS and MS/MS, respectively. All peaks were resolved monoisotopically.

Tandem MS/MS data from LC-ESI-MS/MS runs were submitted to the search engine Mascot to identify the tryptic peptides of CP. One missed cleavage was allowed, and tolerances of 2.0 and 0.8 u mass were used for precursor and product ions, respectively. From the data for LC-ESI-MS/MS at *m/z* 1000–2000, glycopeptide precursor ions were selected manually based on the presence of oligosaccharide oxonium ions such as *m/z* 204 (HexNAc) and *m/z* 366 (HexHexNAc). The glycopeptide ions were assigned based on

the presence of b- and y-series fragment ions of peptides of putative glycopeptides or molecular weight difference of sugar unit. The molecular weight of the carbohydrate in the glycopeptide was calculated from the molecular weights of the glycopeptide and the suggested peptide. The oligosaccharide composition and type were deduced from the molecular weight of the carbohydrate.

Oligosaccharide sequencing by exoglycosidase digestions

Trypsin in the digest of human CP was inactivated by boiling for 5 min at 100 °C. Aliquots of the digest (4 μg) were digested in a volume of 20 μl for 12 h at 37 °C in 50 mM sodium phosphate buffer (pH 5.0) using the following exoglycosidases alone or in combination: α2–3 neuraminidase, 20 mU/ml; α2–3,6,8,9 neuraminidase, 100 mU/ml; α1–3,4 fucosidase, 20 mU/ml; and β1–4 galactosidase, 30 mU/ml. Aliquots (0.08 μg) before and after exoglycosidase digestions were subjected to LC-ESI-MS at *m/z* 700 to 2000 in which MS/MS acquisition was not performed.

Results

Peptide mapping of tryptic digest of human CP (LC-ESI-MS/MS in m/z range of 400–2000)

The amino acid sequence of human CP (National Center for Biotechnology Information protein database: P00450) is shown in Fig. 1. The tryptic peptides, including potential N-glycosylation sites, are shown in bold type. Trypsin can digest human CP into seven glycopeptides containing only one potential N-glycosylation site. To determine the glycosylation state at each glycosylation site, we performed mass spectrometric peptide mapping of the tryptic digest of CP. An aliquot of 0.2 μg of the tryptic digest was analyzed by

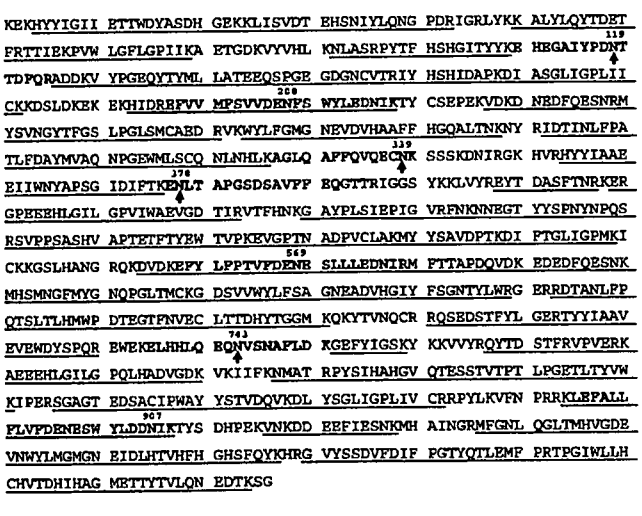

Fig. 1. Primary amino acid sequence of human CP (P00450). The tryptic peptides, including potential N-glycosylation sites, are shown in bold type. Tryptic peptides identified in the LC-ESI-MS/MS analysis are underlined. Cysteine residues are carboxymethylated. Identified N-glycosylation sites are indicated by arrow.

LC-ESI-MS/MS in the *m/z* range of 400–2000 (data not shown). When molecular ions with more than a single charge were detected, the product ion spectrum was acquired automatically. Peptide identification of each product ion spectrum was done using the Mascot search engine. More than 70% of the amino acid sequence was identified; identified amino acids of CP are underlined in Fig. 1. Three peptides containing the potential N-glycosylation site (Asn208, Asn569, and Asn907 [residues 197–218, 558–579, and 895–917, respectively]) were detected, whereas peptides containing the other N-glycosylation sites were not detected. Thus, Asn119, Asn339, Asn378, and Asn743 might be glycosylated.

Glycosylation analysis of human CP (LC-ESI-MS/MS in the m/z range of 1000–2000)

N-glycosylated peptides have relatively high molecular weights due to their oligosaccharide moiety. Because ions at lower *m/z* values can be detected in the *m/z* range of 400–2000, glycopeptide ions with higher *m/z* values might be missed to obtain product ion spectra. To detect glycopeptide ions preferentially, another LC-ESI-MS/MS analysis was carried out in the *m/z* range of 1000–2000 using an aliquot of 0.4 μg of the tryptic digest. Fig. 2A shows a total ion chromatogram (TIC) of a TOF-MS scan for the full scan *m/z* 1000–2000. Fig. 2B shows a TIC of the product ion scan. Because product ion spectra of glycopeptide precursor ions have abundant carbohydrate B-ions, *m/z* 204 (HexNAc), *m/z* 186 (HexNAc-H_2O), *m/z* 366 (HexHexNAc), and *m/z* 292 (NeuAc), the extracted ion chromatogram at *m/z* 204.05–204.15 (HexNAc, 204.08) of the product ion scan is illustrated in Fig. 2C. The extracted ion chromatogram at *m/z* 204.05–204.15 of product ion spectra provides a useful indication of the selection of glycopeptide precursor ions. The glycopeptide ions were assigned based on an examination of product ion spectra using the information on amino acid sequences of the peptides containing a putative N-glycosylation site.

Identification of Asn119 glycopeptide

The product ion spectrum of 1366.6 (+3) at 26 min, labeled by A in Fig. 2C, is shown in Fig. 3A. There were abundant oligosaccharide oxonium ions such as *m/z* 204 (HexNAc), *m/z* 366 (HexHexNAc), *m/z* 186 (HexNAc-H_2O), *m/z* 168 (HexNAc-$2H_2O$), *m/z* 274 (NeuAc-H_2O), and *m/z* 292 (NeuAc). Thus, this precursor ion was assigned as a glycopeptide. Several fragment ions consistent with b- and y-series fragment ions [24] derived from the peptide EHEGAIYPDN^{119}TTDFQR (residues 110–125) were detected together with several deamidated (−17) or dehydrogenated (−18) b- and y-series ions and y-series ions with the GlcNAc residue. Thus, the peptide moiety EHEGA IYPDNTTDFQR was suggested. The carbohydrate's molecular weight, 2223.0, was calculated by subtracting the theoretical molecular weight of the peptide (1891.8) from

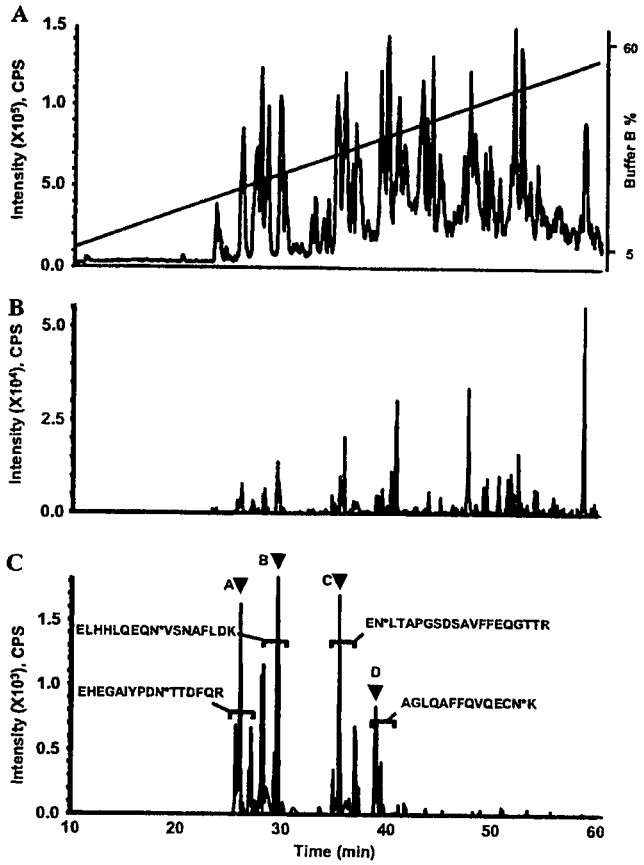

Fig. 2. LC-ESI-MS/MS in the *m/z* range of 1000–2000 of the tryptic digest of human CP. (A) TIC of the TOF-MS scan for the full-scan *m/z* 1000–2000 and the HPLC gradient. (B) TIC of the product ion scan acquired data-dependently. (C) Extracted ion chromatograph at *m/z* 204.05–204.15 of the product ion spectra. Brackets denote glycopeptide fraction and peptide sequences of the glycopeptides. Product ion spectra indicated by A–D are shown in Fig. 3.

the calculated molecular weight of the glycopeptide (4096.7) and adding the molecular weight of H_2O (18.0). The presence of product ions at *m/z* 274 (NeuAc-H_2O) and *m/z* 292 (NeuAc) suggested sialylation of the oligosaccharide. Thus, the carbohydrate's composition, $[HexNAc]_4[Hex]_5[NeuAc]_2$, was deduced.

Identification of Asn743 glycopeptide

The product ion spectrum of 1628.4 (+3) at 29 min, labeled by B in Fig. 2C, is shown in Fig. 3B. This precursor ion was assigned as a glycopeptide due to the presence of abundant oligosaccharide oxonium ions such as *m/z* 204 (HexNAc), *m/z* 366 (HexHexNAc), and *m/z* 292 (NeuAc) in the product ion spectrum. Several fragment ions were consistent with theoretical b- and y-series fragment ions derived from the peptide ELHHLQEQN^{743}VSNAFLDK (residues 735–751). Doubly charged ions of peptide (*m/z* 1011.7), peptide + HexNAc (*m/z* 1113.1), peptide + 2HexNAc (*m/z* 1214.6), peptide + 2HexNAc + Hex (*m/z* 1295.5), peptide + 2HexNAc + 2Hex (*m/z* 1376.7), and peptide + 2HexNAc + 3Hex (*m/z* 1457.5) showed the sequential fragmentation of the pentasaccharide carbohydrate core. The carbohydrate's molecular weight, 2879.1, was calculated from the theoretical molecular weight of the peptide (2021.0) and the calculated molecular weight of the glycopeptide (4882.1). The carbohydrate's composition, $[HexNAc]_5[Hex]_6[NeuAc]_3$, was deduced from the molecular weight.

Identification of Asn378 glycopeptide

The product ion spectrum of 1444.6 (+3) at 35 min, labeled by C in Fig. 2C, is shown in Fig. 3C. Abundant oligosaccharide oxonium ions were detected, as were several fragment ions consistent with b- and y-series fragment ions derived from the peptide EN^{378}LTAPGSDSAVFFEQGT TR (residues 377–391). The carbohydrate's molecular weight, 2222.9, was calculated from the theoretical molecular weight of the peptide (2126.0) and the calculated molecular weight of the glycopeptide (4330.9). Thus, the peptide moiety ENLTAPGSDSAVFFEQGTTR and the carbohydrate's composition, $[HexNAc]_4[Hex]_5[NeuAc]_2$, were suggested.

Identification of Asn339 glycopeptide

The product ion spectrum of 1282.6 (+3) at 39 min, labeled by D in Fig. 2C, is shown in Fig. 3C. The spectrum contains abundant oligosaccharide oxonium ions, and several fragment ions consistent with b- and y-series fragment ions derived from the peptide AGLQAFFQVQECN^{339}K (residues 327–340) were detected. The product ion spectrum contains the ions of the peptide (*m/z* 1640.8) and peptide + HexNAc (*m/z* 1843.9) and several y-series fragment ions of the peptide with a GlcNAc residue. The carbohydrate's molecular weight, 2223.0, was calculated from the theoretical molecular weight of the peptide (1639.7) and the calculated molecular weight of the glycopeptide (3844.7). Thus, the peptide moiety AGLQAFFQVQECNK and the carbohydrate's composition, $[HexNAc]_4[Hex]_5[NeuAc]_2$, were suggested.

Heterogeneity of oligosaccharides at each glycosylation site

Glycopeptides with the potential N-glycosylation sites Asn119, Asn339, Asn378, and Asn743 were detected, whereas no glycopeptides containing the other sites (Asn208, Asn569, and Asn907) could be detected in this LC-ESI-MS/MS analysis. These findings suggest that Asn119, Asn339, Asn378, and Asn743 of human CP are glycosylated and that Asn208, Asn569, and Asn907 are not. Once a glycopeptide was identified, the other glycopeptides with the same peptide could be easily assigned because they were eluted at a similar retention time in the order of the number of NeuAc and had similar product ion spectra and molecular weight difference of sugar units. The oligosaccharide heterogeneity at each four N-glycosylation sites was determined by mass spectrum. For a representative example, the mass spectrum of the glycopeptides containing

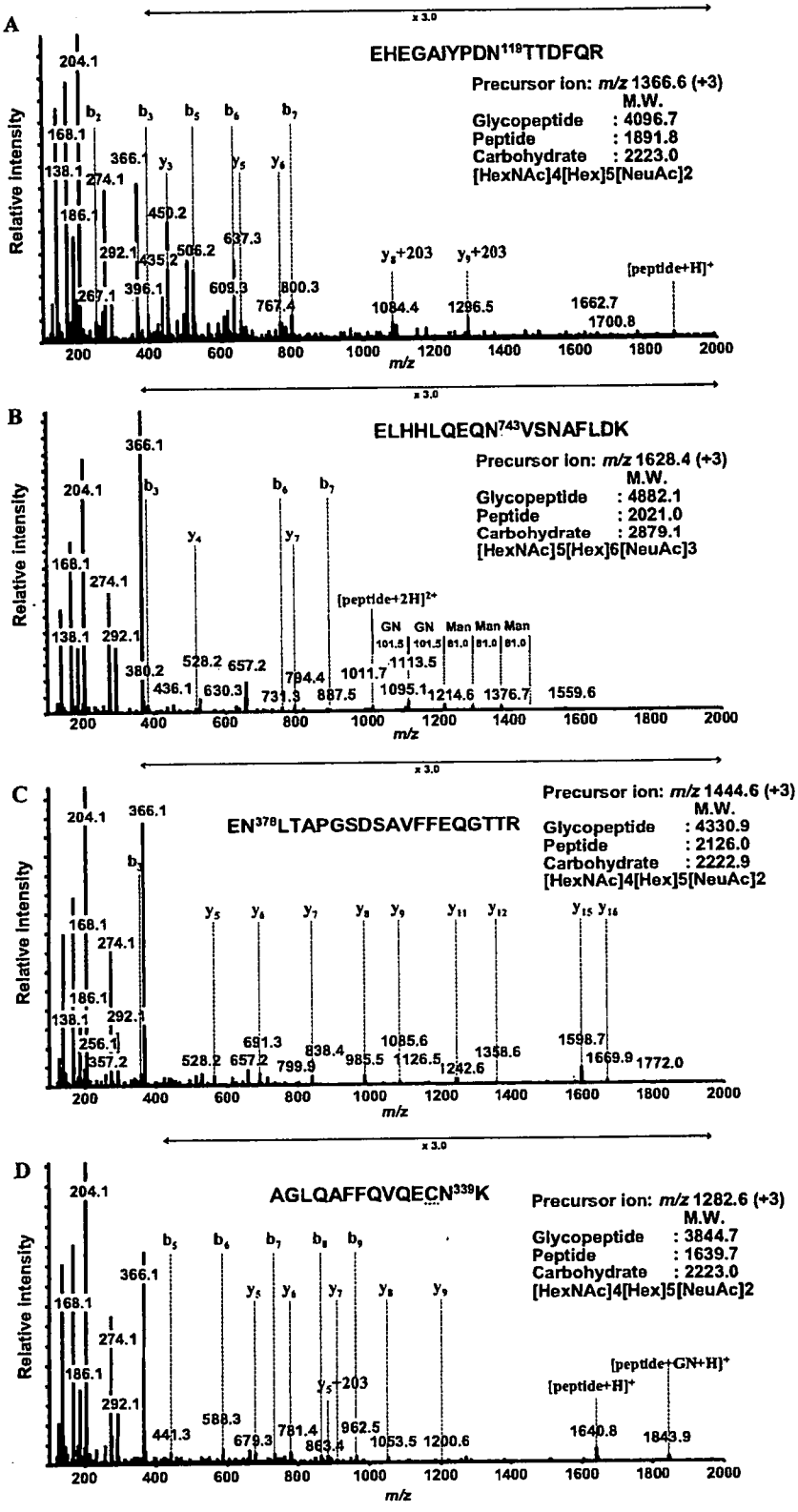

Fig. 3. Product ion spectra of *m/z* 1366.6 (+3) at 26 min (A), *m/z* 1628.4 (+3) at 29 min (B), *m/z* 1444.6 (+3) at 35 min (C), and *m/z* 1282.6 (+3) at 39 min (D) labeled by A, B, C, and D, respectively, in Fig. 2C. These spectra show abundant carbohydrate-derived ions at *m/z* 168 (HexNAc-2H_2O), *m/z* 186 (HexNAc-H_2O), *m/z* 204 (HexNAc), *m/z* 366 (HexHexNAc), *m/z* 274 (NeuAc-H_2O), and *m/z* 292 (NeuAc). The b- and y-series fragment ions [24] derived from the peptide moiety were observed. The molecular weights of the oligosaccharide were calculated from the molecular weights of the glycopeptide and peptide, and the deduced oligosaccharide composition is presented. Cystein residue was carboxymethylated.

Asn743 at 27.5 to 31.5 min is shown Fig. 4. The results of glycosylation analysis are summarized in Table 1. Deduced compositions of the oligosaccharides are estimated based on the calculated molecular weights of the oligosaccharides. Relative peak intensity was calculated by comparing triply charged glycopeptide ions. All glycosylation sites were occupied by at least three kinds of oligosaccharides, namely disialobiantennary structures ($[HexNAc]_4[Hex]_5[NeuAc]_2$), disialobiantennary structures with fucose ($[HexNAc]_4[Hex]_5[NeuAc]_2[Fuc]_1$), and trisialotriantennary structures ($[HexNAc]_5[Hex]_6[NeuAc]_3$). Trisialotriantennary structures with one fucose or two fucoses ($[HexNAc]_5[Hex]_6[NeuAc]_3[Fuc]_{1-2}$) were also detected at Asn119 and Asn743; furthermore, tetrasialotetraantennary structures with no fucose or one fucose ($[HexNAc]_6[Hex]_7[NeuAc]_4[Fuc]_{0-1}$) were detected at Asn743.

Linkage analysis of oligosaccharides by exoglycosydase digestion

To elucidate the oligosaccharide structure in terms of sequence and linkage, aliquots of the tryptic digest were further digested with exoglycosidases. As a representative example, Fig. 5 shows integrated mass spectra during the periods at which Asn119 glycopeptides were eluted in LC-ESI-MS analyses before and after digestion with exoglycosidase arrays. Treatment with α2–3 neuraminidase removed one NeuAc residue from most of the triantennary structures ($[HexNAc]_5[Hex]_6[NeuAc]_3[Fuc]_{0-2}$) and a small amount of biantennary structures ($[HexNAc]_4[Hex]_5[NeuAc]_2[Fuc]_{0-1}$) (Fig. 5B). A minor amount of triantennary structures removed two NeuAc residues. Thus, it appears that most triantennary structures contain one α2–3-linked NeuAc. Treatment with α2–3 neuraminidase + β1–4 galactosidase removed all terminal galactose residues from the desialylated glycans without fucose residues but only partially digested terminal galactoses from the desialylated glycans with fucoses (Fig. 5C). The addition of α1–3,4 fucosidase to α2–3 neuraminidase + β1–4 galactosidase treatment completely digested the remaining terminal galactose by releasing one fucose and one galactose (Fig. 5D). Thus, galactose residues are linked β1–4 to GlcNAc, and undigestion of terminal galactose by β1–4 galactosidase is due to attachment of fucose [25,26]. Because galactose was linked to GlcNAc in the β1–4 position, the fucose removed with α1–3,4 fucosidase may be linked α1–3 to GlcNAc but not α1–4 to GlcNAc. These data strongly suggested that sialyl Lewis X structure was present in human CP. Sialyl Lewis X structure was present predominantly in triantennary oligosaccharides, but a small amount seemed to be present in biantennary oligosaccharides as well. The remaining fucose residue may be linked α1–6 to reducing end GlcNAc (core fucose).

Fig. 6 shows integrated mass spectra of Asn119, Asn743, Asn378, and Asn339 glycopeptides in LC-ESI-MS analysis following digestion with α2–3,6,8,9 neuraminidase + β1–4 galactosidase. Treatment with α2–3,6,8,9 neuraminidase + β1–4 galactosidase removed all NeuAc and then removed terminal galactoses in the outer arms without fucose. Thus, this treatment could differentiate glycoforms based on the location of fucose residues. Fucosylation occurred predominantly at reducing end GlcNAc in biantennary oligosaccharides and occurred at reducing end GlcNAc and/or outer arm GlcNAc in triantennary oligosaccharides. Mass spectra of Asn119 and Asn743 glycopeptides showed higher oligosaccharide heterogeneity, and a minor amount of tetraantennary glycans could be detected. The glycosylation profile

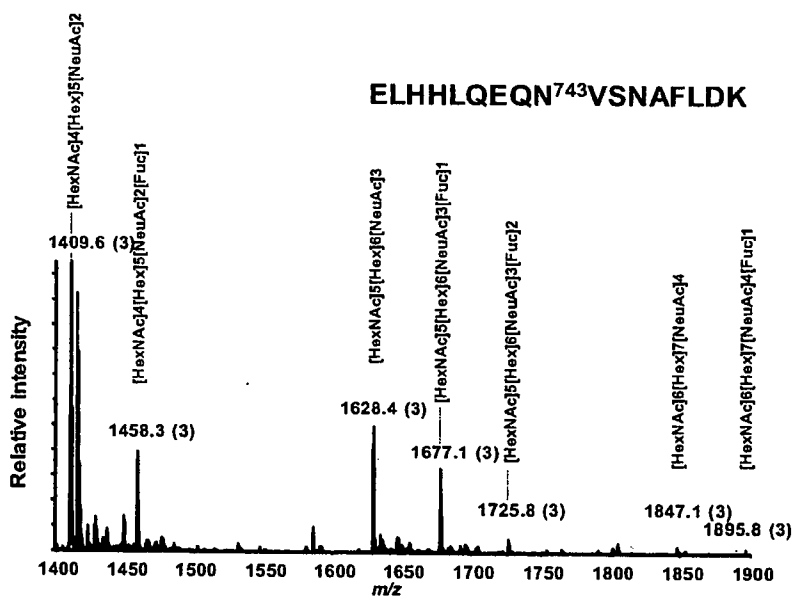

Fig. 4. Mass spectrum of the glycopeptides containing Asn743 eluting at 27.5–31.5 min from Fig. 2A. Deduced composition of the oligosaccharides is indicated based on the molecular weights of the oligosaccharides.

Table 1
Results of site-specific glycosylation analysis of human CP

Retention time (min)	Glycopeptides		Calculated MW	Relative peak intensity[a] (%)	Peptide		Oligosaccharide		
	m/z	Charge			Sequence	Theoretical MW	Calculated MW	Theoretical MW	Composition[b,c]
26	1415.3	+3	4242.8	52	EHEGAIYPDN[119]TTDFQR	1891.8	2369.0	2368.8	[HexNAc]4[Hex]5[NeuAc]2[Fuc]1
26	1366.6	+3	4096.7	100	EHEGAIYPDN[119]TTDFQR	1891.8	2223.0	2222.8	[HexNAc]4[Hex]5[NeuAc]2
27	1682.7	+3	5045.1	6	EHEGAIYPDN[119]TTDFQR	1891.8	3171.3	3171.1	[HexNAc]5[Hex]6[NeuAc]3[Fuc]2
27	1634.0	+3	4899.0	21	EHEGAIYPDN[119]TTDFQR	1891.8	3025.2	3025.1	[HexNAc]5[Hex]6[NeuAc]3[Fuc]1
27	1225.8	+4	4899.0						
27	1585.3	+3	4753.0	24	EHEGAIYPDN[119]TTDFQR	1891.8	2879.2	2879.0	[HexNAc]5[Hex]6[NeuAc]3
27	1189.3	+4	4753.0						
28	1458.3	+3	4372.0	35	ELHHLQEQN[743]VSNAFLDK	2021.0	2369.0	2368.8	[HexNAc]4[Hex]5[NeuAc]2[Fuc]1
28	1409.6	+3	4225.9	100	ELHHLQEQN[743]VSNAFLDK	2021.0	2222.9	2222.8	[HexNAc]4[Hex]5[NeuAc]2
28	1057.5	+4	4225.9						
29	1725.8	+3	5174.5	5	ELHHLQEQN[743]VSNAFLDK	2021.0	3171.5	3171.1	[HexNAc]5[Hex]6[NeuAc]3[Fuc]2
29	1294.6	+4	5174.2						
29	1677.1	+3	5028.2	29	ELHHLQEQN[743]VSNAFLDK	2021.0	3025.3	3025.1	[HexNAc]5[Hex]6[NeuAc]3[Fuc]1
29	1258.1	+4	5028.2						
29	1628.4	+3	4882.1	43	ELHHLQEQN[743]VSNAFLDK	2021.0	2879.1	2879.0	[HexNAc]5[Hex]6[NeuAc]3
29	1221.5	+4	4882.1						
31[d]	1895.8	+3	5684.4	2	ELHHLQEQN[743]VSNAFLDK	2021.0	3681.4	3681.3	[HexNAc]6[Hex]7[NeuAc]4[Fuc]1
31[d]	1422.1	+4	5684.3						
31[d]	1847.1	+3	5538.4	3	ELHHLQEQN[743]VSNAFLDK	2021.0	3535.4	3535.2	[HexNAc]6[Hex]7[NeuAc]4
31	1385.6	+4	5538.3						
35[d]	1493.3	+3	4477.0	6	EN[378]LTAPGSDSAVFFEQGTTR	2126.0	2369.0	2368.8	[HexNAc]4[Hex]5[NeuAc]2[Fuc]1
35	1444.6	+3	4330.9	100	EN[378]LTAPGSDSAVFFEQGTTR	2126.0	2222.9	2222.8	[HexNAc]4[Hex]5[NeuAc]2
37	1712.1	+3	5133.2	8	EN[378]LTAPGSDSAVFFEQGTTR	2126.0	3025.2	3025.1	[HexNAc]5[Hex]6[NeuAc]3[Fuc]1
37	1284.3	+4	5133.2						
37	1663.4	+3	4987.1	23	EN[378]LTAPGSDSAVFFEQGTTR	2126.0	2879.2	2879.0	[HexNAc]5[Hex]6[NeuAc]3
37	1247.8	+4	4987.2						
39	1331.3	+3	3990.8	14	AGLQAFFQVQECN[339]K	1639.7	2369.1	2368.8	[HexNAc]4[Hex]5[NeuAc]2[Fuc]1
39	1923.4	+2	3844.7		AGLQAFFQVQECN[339]K	1639.7	2223.0	2222.8	[HexNAc]4[Hex]5[NeuAc]2
39	1282.6	+3	3844.7	100					
41	1501.3	+3	4500.8	6	AGLQAFFQVQECN[339]K	1639.7	2879.2	2879.0	[HexNAc]5[Hex]6[NeuAc]3

Note. All masses are monoisotopic. Cysteine residue was carboxymethylated.

[a] Relative peak intensity was calculated by comparing same charge state glycopeptide ions. The intensity of the glycoform with maximum at each glycosylation site was taken as 100%.

[b] The oligosaccharide composition was deduced from the molecular weight of the oligosaccharide.

[c] The glycopeptide ions adducted by NH_4^+ or Na^+ were excluded.

[d] Product ion spectra of these molecular ions were not acquired. However, these were considered glycopeptides because of a molecular weight difference of 146 (Fuc) and the same retention time as other glycopeptides.

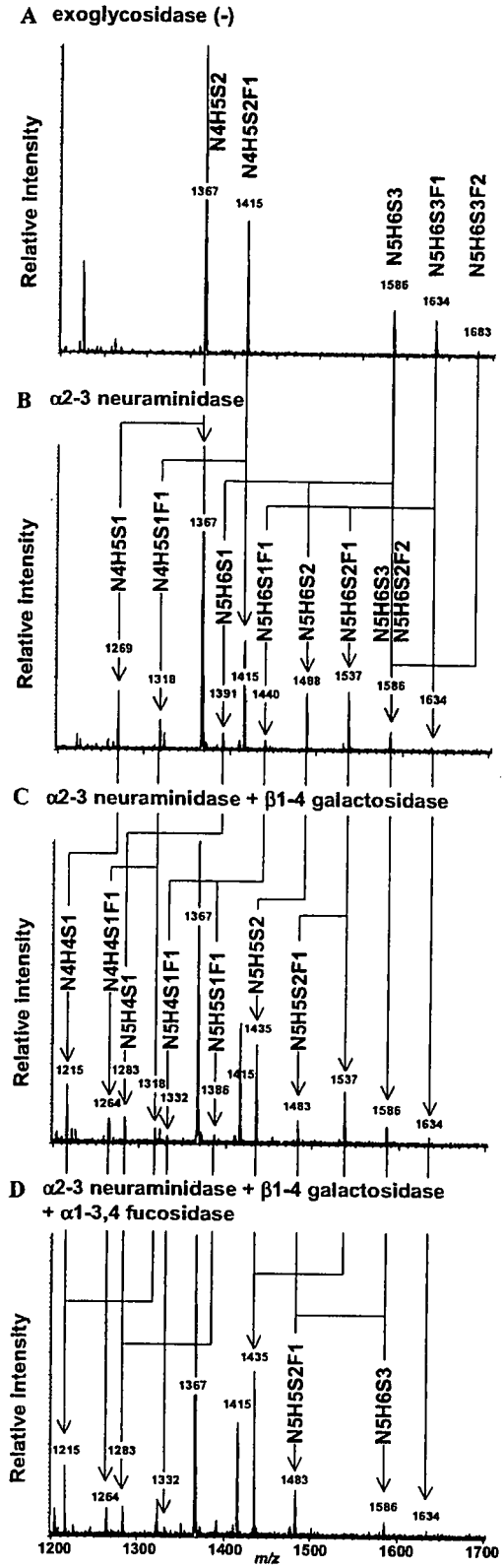

Fig. 5. LC-ESI mass spectra of the glycopeptides containing Asn119 digested with the following exoglycosidases: (A) exoglycosidase (–); (B) α2–3 neuraminidase; (C) α2–3 neuraminidase + β1–4 galactosidase; (D) α2–3 neuraminidase + β1–4 galactosidase + α1–3,4 fucosidase. Arrows between panels A and B, panels B and C, and panels C and D correspond to the digestion of NeuAc, Gal, and Gal+Fuc, respectively. H, hexose; N, *N*-acetylhexosamine; F, fucose; S, *N*-acetylneuraminic acid.

of Asn378 glycopeptides showed lower core fucosylation, and that of Asn339 glycopeptides showed lower branching. These glycosylation profiles provided the heterogeneity of fucose linkage and the number of arms at each glycosylationsite in human CP.

Discussion

A site-specific glycosylation analysis of human CP was conducted using LC-ESI-MS/MS, where product ion spectra were acquired in a data-dependent manner. The collision energy for the product ion scan was adjusted from 30 to 80 eV depending on the size and charge of the precursor ion. Under these conditions, peptide precursor ions were degraded and produced b- and y-series fragment ions derived from the amino acid sequence. Glycopeptide precursor ions produced abundant carbohydrate ions (*m/z* 204, 186, 168, and 366) together with several low intensity b- and y-series fragment ions derived from the amino acid sequence [20,21]. Thus, product ion spectra of glycopeptides are readily distinguishable from those of peptides by such carbohydrate marker ions, and the peptide moiety in the glycopeptide could be deduced from the product ions that were consistent with the expected fragment ions derived from the peptide containing the N-glycosylation site. It is known that the glycopeptide ions are more labile than peptide ions and produce consecutive monosaccharide/polysaccharide losses at much lower collision energy, and this would provide information about branching and fucose location [18]. However, we used relatively high collision energy in this site-specific glycosylation analysis to identify the peptide ions in parallel with the detection and identification of the glycopeptide ions.

Protein coverage of more than 70% in human CP was obtained in the LC-ESI-MS/MS analysis with the *m/z* range of 400–2000 (for peptide mapping). The heterogeneity at four potential N-glycosylation sites was determined in the *m/z* range of 1000–2000 (glycosylation analysis). We could detect all of the potential glycosylation sites as either glycopeptides or nonglycosylated peptides. Peptides containing the potential N-glycosylation site Asn208, Asn569, or Asn907 were detected in nonglycosylated but not glycosylated forms. Peptides with the potential N-glycosylation site Asn119, Asn339, Asn378 or Asn743 were detected in glycosylated but not nonglycosylated forms. These findings indicate that Asn119, Asn339, Asn378, and Asn743 of human CP are glycosylated and that Asn208, Asn569, and Asn907 are not. Human CP was reported to have no O-linked glycosylation [8]. No information on O-glycosylation was obtained from this analysis. These results are consistent with a previous study determining the glycosylation sites of human CP [9].

Heterogeneity of oligosaccharides was determined at each of four glycosylation sites. Disialobiantennary structures with no fucose or one fucose ($[HexNAc]_4$ $[Hex]_5$ $[NeuAc]_2[Fuc]_{0-1}$) and trisialotriantennary structures

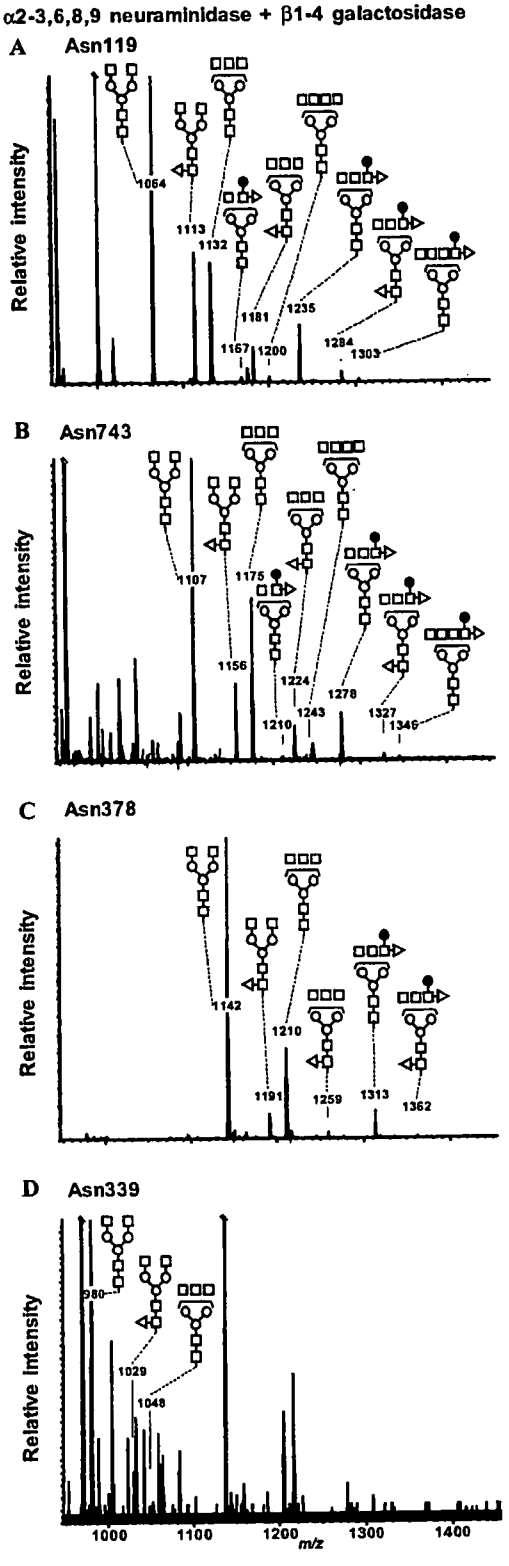

Fig. 6. LC-ESI mass spectra of the glycopeptides containing Asn119 (A), Asn743 (B), Asn378 (C), and Asn339 (D) after digestion with α2–3,6,8,9 neuraminidase + β1–4 galactosidase. Glycosylation profiles showed different degrees of branching and fucosylation at core GlcNAc and outer arm GlcNAc between glycosylation sites. Open circles, mannose; closed circles, galactose; open squares, *N*-acetyl glucosamine; open triangles, fucose.

($[HexNAc]_5[Hex]_6[NeuAc]_3$) were observed at all sites. These dominant oligosaccharides were consistent with structures published previously [7,8]. Furthermore, we detected trisialotriantennary structures with one fucose ($[HexNAc]_5[Hex]_6[NeuAc]_3[Fuc]_1$) at Asn119, Asn378, and Asn743, trisialotriantennary structures with two fucoses ($[HexNAc]_5[Hex]_6[NeuAc]_3[Fuc]_2$) at Asn119 and Asn743, and tetrasialotetraantennary structures with no fucose or one fucose ($[HexNAc]_6[Hex]_7[NeuAc]_4[Fuc]_{0-1}$) at Asn743.

To determine the linkage of fucose and NeuAc, exoglycosidase digestions were performed. Treatment with α2–3 neuraminidase suggested that roughly one antenna of triantennary glycans was linked by NeuAc in the α2–3 position. This is consistent with the previous findings that NeuAc is linked α2–3 to the Galβ1–4GlcNAcβ1–4Manα1–3Manβ1–4GlcNAcβ1–4GlcNAc group in the triantennary glycan in human CP [7,8]. Results from α2–3 neuraminidase + β1–4 galactosidase treatments with or without α1–3,4 fucosidase suggested that fucose residues were linked to reducing end GlcNAc and/or outer arm GlcNAc in the α1–3 position in the antenna where NeuAc is linked to galactose in the α2–3 position. These findings indicated that human CP contains a certain amount of sialyl Lewis X structure in triantennary glycans. Treatment with α2–3,6,8,9 neuraminidase + β1–4 galactosidase reveals the heterogeneity of the location of fucosylation as well as the number of arms. Although relative peak intensity does not express the relative amount of each glycan due to the different ionization efficiencies, the mass spectra showed the difference in fucosylation pattern and number of arms among sites.

No asialo oligosaccharides were detected in this analysis. It is known that desialylated CP is rapidly cleared from the circulation by the asialoglycoprotein receptor within the parenchymal cells of liver [27,28]. It is possible that desialylated CP might be cleared immediately by the liver.

Although the N-linked carbohydrate structures linked to human CP have been studied, only a few carbohydrate structures have been reported and site-specific characterization of these oligosaccharides has not been described. To determine the glycosylation state at each glycosylation site, the tryptic digest was examined by LC-ESI-MS/MS, where product ion spectra were acquired data-dependently. Glycopeptide ions were assigned based on the product ion spectra. Fucose and NeuAc linkages were determined by exoglycosidase digestions. Our data successfully provided comprehensive information on the site-specific N-linked oligosaccharides in human CP. This method is a powerful technique for elucidating the glycosylation of a biological sample.

Acknowledgments

This study was supported by a Grant-in-Aid for Research on Health Sciences focusing on Drug Innovation from the Japan Health Sciences Foundation.

References

[1] S. Osaki, D.A. Johnson, E. Frieden, The possible significance of the ferrous oxidase activity of ceruloplasmin in normal human serum, J. Biol. Chem. 241 (1966) 2746–2751.

[2] K. Yoshida, K. Furihata, S. Takeda, A. Nakamura, K. Yamamoto, H. Morita, S. Hiyamuta, S. Ikeda, N. Shimizu, N. Yanagisawa, A mutation in the ceruloplasmin gene is associated with systemic hemosiderosis in humans, Nat. Genet. 9 (1995) 267–272.

[3] Z.L. Harris, Y. Takahashi, H. Miyajima, M. Serizawa, R.T. MacGillivray, J.D. Gitlin, Aceruloplasminemia: molecular characterization of this disorder of iron metabolism, Proc. Natl. Acad. Sci. USA 92 (1995) 2539–2543.

[4] Z.L. Harris, A.P. Durley, T.K. Man, J.D. Gitlin, Targeted gene disruption reveals an essential role for ceruloplasmin in cellular iron efflux, Proc. Natl. Acad. Sci. USA 96 (1996) 10812–10817.

[5] N. Takahashi, T.L. Ortel, F.W. Putnam, Single-chain structure of human ceruloplasmin: the complete amino acid sequence of the whole molecule, Proc. Natl. Acad. Sci. USA 81 (1984) 390–394.

[6] M.L. Koschinsky, W.D. Funk, B.A. van Oost, R.T. MacGillivray, Complete cDNA sequence of human preceruloplasmin, Proc. Natl. Acad. Sci. USA 83 (1986) 5086–5090.

[7] K. Yamashita, C.J. Liang, S. Funakoshi, A. Kobata, Structural studies of asparagine-linked sugar chains of human ceruloplasmin. Structural characteristics of the triantennary complex type sugar chains of human plasma glycoproteins, J. Biol. Chem. 256 (1981) 1283–1289.

[8] M. Endo, K. Suzuki, K. Schmid, B. Fournet, Y. Karamanos, J. Montreuil, L. Dorland, H. van Halbeek, J.F. Vliegenthart, The structures and microheterogeneity of the carbohydrate chains of human plasma ceruloplasmin: a study employing 500-MHz ^{1}H-NMR spectroscopy, J. Biol. Chem. 257 (1982) 8755–8760.

[9] N. Takahashi, Y. Takahashi, T.L. Ortel, J.N. Lozier, N. Ishioka, F.W. Putnam, Purification of glycopeptides of human plasma proteins by high-performance liquid chromatography, J. Chromatogr. 317 (1984) 11–26.

[10] R.J. Cousins, Absorption, transport, and hepatic metabolism of copper and zinc: special reference to metallothionein and ceruloplasmin, Physiol. Rev. 65 (1985) 238–309.

[11] A. Mackiewicz, M.K. Ganapathi, D. Schultz, I. Kushner, Monokines regulate glycosylation of acute-phase proteins, J. Exp. Med. 166 (1987) 253–258.

[12] J.E. Hansen, J. Iversen, A. Lihme, T.C. Bog-Hansen, Acute phase reaction, heterogeneity, and microheterogeneity of serum proteins as nonspecific tumor markers in lung cancer, Cancer 60 (1987) 1630–1635.

[13] A. Senra Varela, J.J. Lopez Saez, D. Quintela Senra, Serum ceruloplasmin as a diagnostic marker of cancer, Cancer Lett. 121 (1997) 139–145.

[14] V. Ling, A.W. Guzzetta, E. Canova-Davis, J.T. Stults, W.S. Hancock, T.R. Covey, B.I. Shushan, Characterization of the tryptic map of recombinant DNA derived tissue plasminogen activator by high-performance liquid chromatography-electrospray ionization mass spectrometry, Anal. Chem. 63 (1991) 2909–2915.

[15] S.A. Carr, M.J. Huddleston, M.F. Bean, Selective identification and differentiation of N- and O-linked oligosaccharides in glycoproteins by liquid chromatography–mass spectrometry, Protein Sci. 2 (1993) 183–196.

[16] M.J. Huddleston, M.F. Bean, S.A. Carr, Collisional fragmentation of glycopeptides by electrospray ionization LC/MS and LC/MS/MS: methods for selective detection of glycopeptides in protein digests, Anal. Chem. 65 (1993) 877–884.

[17] P.A. Schindler, C.A. Settineri, X. Collet, C.J. Fielding, A.L. Burlingame, Site-specific detection and structural characterization of the glycosylation of human plasma proteins lecithin:cholesterol acyltransferase and apolipoprotein D using HPLC/electrospray mass spectrometry and sequential glycosidase digestion, Protein Sci. 4 (1995) 791–803.

[18] M.A. Ritchie, A.C. Gill, M.J. Deery, K. Lilley, Precursor ion scanning for detection and structural characterization of heterogeneous glycopeptide mixtures, J. Am. Soc. Mass Spectrom. 13 (2002) 1065–1077.

[19] F. Wang, A. Nakouzi, R.H. Angeletti, A. Casadevall, Site-specific characterization of the N-linked oligosaccharides of a murine immunoglobulin M by high-performance liquid chromatography/electrospray mass spectrometry, Anal. Biochem. 314 (2003) 266–280.

[20] J.F. Nemeth, G.P. Hochgesang Jr., L.J. Marnett, R.M. Caprioli, Characterization of the glycosylation sites in cyclooxygenase-2 using mass spectrometry, Biochemistry 40 (2001) 3109–3116.

[21] O. Krokhin, W. Ens, K.G. Standing, J. Wilkins, H. Perreault, Site-specific N-glycosylation analysis: matrix-assisted laser desorption/ionization quadrupole–quadrupole time-of-flight tandem mass spectral signatures for recognition and identification of glycopeptides, Rapid Commun. Mass Spectrom. 18 (2004) 2020–2030.

[22] A. Harazono, N. Kawasaki, T. Kawanishi, T. Hayakawa, Site-specific glycosylation analysis of human apolipoprotein B100 using LC/ESI MS/MS, Glycobiology 15 (2005) 447–462.

[23] C.W. Sutton, J.A. O'Neill, J.S. Cottrell, Site-specific characterization of glycoprotein carbohydrates by exoglycosidase digestion and laser desorption mass spectrometry, Anal. Biochem. 218 (1994) 34–46.

[24] P. Roepstorff, J. Fohlman, Proposal for a common nomenclature for sequence ions in mass spectra of peptides, Biomed. Mass Spectrom. 11 (1984) 601.

[25] K. Maemura, M. Fukuda, Poly-*N*-acetyllactosaminyl *O*-glycans attached to leukosialin: the presence of sialyl Le(x) structures in *O*-glycans, J. Biol. Chem. 267 (1992) 24379–24386.

[26] S. Hemmerich, S.D. Rosen, 6'-Sulfated sialyl Lewis X is a major capping group of GlyCAM-1, Biochemistry 33 (1994) 4830–4835.

[27] C.J. Van Den Hamer, A.G. Morell, I.H. Scheinberg, J. Hickman, G. Ashwell, Physical and chemical studies on ceruloplasmin: IX. The role of galactosyl residues in the clearance of ceruloplasmin from the circulation, J. Biol. Chem. 245 (1970) 4397–4402.

[28] A.G. Morell, G. Gregoriadis, I.H. Scheinberg, J. Hickman, G. Ashwell, The role of sialic acid in determining the survival of glycoproteins in the circulation, J. Biol. Chem. 246 (1971) 1461–1467.

The EMBO Journal (2006) 25, 5305–5316 | © 2006 European Molecular Biology Organization | All Rights Reserved 0261-4189/06
www.embojournal.org

THE EMBO JOURNAL

TRPC3 and TRPC6 are essential for angiotensin II-induced cardiac hypertrophy

Naoya Onohara[1], Motohiro Nishida[1], Ryuji Inoue[2], Hiroyuki Kobayashi[1], Hideki Sumimoto[3], Yoji Sato[4], Yasuo Mori[5], Taku Nagao[4] and Hitoshi Kurose[1,*]

[1]Department of Pharmacology and Toxicology, Graduate School of Pharmaceutical Sciences, Kyushu University, Higashi-ku, Fukuoka, [2]Department of Physiology, School of Medicine, Fukuoka University, Jonan-ku, Fukuoka, Japan, [3]Medical Institute of Bioregulation, Kyushu University, Higashi-ku, Fukuoka, Japan, [4]National Institute of Health Sciences, Setagaya, Tokyo, Japan and [5]Laboratory of Molecular Biology, Department of Synthetic Chemistry and Biological Chemistry, Graduate School of Engineering, Kyoto University, Kyoto, Japan

Angiotensin (Ang) II participates in the pathogenesis of heart failure through induction of cardiac hypertrophy. Ang II-induced hypertrophic growth of cardiomyocytes is mediated by nuclear factor of activated T cells (NFAT), a Ca^{2+}-responsive transcriptional factor. It is believed that phospholipase C (PLC)-mediated production of inositol-1,4,5-trisphosphate (IP_3) is responsible for Ca^{2+} increase that is necessary for NFAT activation. However, we demonstrate that PLC-mediated production of diacylglycerol (DAG) but not IP_3 is essential for Ang II-induced NFAT activation in rat cardiac myocytes. NFAT activation and hypertrophic responses by Ang II stimulation required the enhanced frequency of Ca^{2+} oscillation triggered by membrane depolarization through activation of DAG-sensitive TRPC channels, which leads to activation of L-type Ca^{2+} channel. Patch clamp recordings from single myocytes revealed that Ang II activated DAG-sensitive TRPC-like currents. Among DAG-activating TRPC channels (TRPC3, TRPC6, and TRPC7), the activities of TRPC3 and TRPC6 channels correlated with Ang II-induced NFAT activation and hypertrophic responses. These data suggest that DAG-induced Ca^{2+} signaling pathway through TRPC3 and TRPC6 is essential for Ang II-induced NFAT activation and cardiac hypertrophy.

The EMBO Journal (2006) **25**, 5305–5316. doi:10.1038/sj.emboj.7601417; Published online 2 November 2006
Subject Categories: signal transduction; molecular biology of disease
Keywords: angiotensin; cardiac hypertrophy; diacylglycerol; L-type Ca^{2+} channel; TRPC

Introduction

Regulators of cardiac function such as vasoactive neurotransmitters and hormones activate phospholipase C (PLC) and thereby generate inositol-1,4,5-trisphosphate (IP_3) and diacylglycerol (DAG). These agonists elevate the concentration of cytoplasmic free Ca^{2+} ($[Ca^{2+}]_i$) in cardiomyocytes, which induces positive inotropic effects on the heart and activates several transcriptional pathways that lead to cardiac hypertrophy (Wilkins and Molkentin, 2004; Woodcock and Matkovich, 2005). NFAT is one of the transcriptional factors regulated by $[Ca^{2+}]_i$ (Crabtree and Olson, 2002). The relevance of the NFAT signaling pathway to cardiac hypertrophy is underscored by the observation that cardiac-targeted transgenic animals expressing constitutively activated forms of either calcineurin or NFAT produced ventricular hypertrophy (Molkentin *et al*, 1998; Taigen *et al*, 2000). The Ca^{2+}-sensitive serine/threonine phosphatase (calcineurin) primarily regulates NFAT activity by rapid dephosphorylation of NFAT proteins and their translocation to the nucleus. A drop in nuclear Ca^{2+} deactivates calcineurin and allows one of several NFAT kinases to rephosphorylate NFAT, causing it to leave the nucleus and thereby inactivating transcription (Timmerman *et al*, 1996; Dolmetsch *et al*, 1997). Therefore, a sustained elevation of $[Ca^{2+}]_i$ is required for NFAT-dependent transcription.

The importance of agonists that activate PLC for cardiac hypertrophy is well established (Molkentin and Dorn, 2001). Many lines of evidence have shown that stimulation of PLC-linked G protein-coupled receptors, such as α_1-adrenergic receptor (Maruyama *et al*, 2002), Ang II receptor (Nishida *et al*, 2005) and endothelin receptor (Arai *et al*, 2003), induce hypertrophic growth of rat cardiac myocytes. More clinically relevant, hypertrophied hearts induced by volume overload are commonly characterized by high levels of IP_3-generating agonists such as Ang II (Dostal *et al*, 1992; Sadoshima *et al*, 1993). Numerous studies have demonstrated the need for sustained or periodic increases in $[Ca^{2+}]_i$ to cause the nuclear localization of NFAT (Dolmetsch *et al*, 1997; Tomida *et al*, 2003). In nonexcitable cells, IP_3 is generally accepted to function as a mediator of sustained Ca^{2+} responses (Timmerman *et al*, 1996; Dolmetsch *et al*, 1997). The sustained Ca^{2+} signaling requires the store-operated Ca^{2+} channel (SOC), which opens in response to depletion of intracellular stores through IP_3 receptor (IP_3R). Therefore, it is currently believed that Ca^{2+} entry through SOC regulates NFAT translocation. In the heart, however, the expression level of IP_3R is much lower than that of ryanodine receptor (Moschella and Marks, 1993). Voltage-dependent L-type Ca^{2+} channel and ryanodine receptor function as the major source of Ca^{2+} for normal Ca^{2+}-induced Ca^{2+} release of excitation–contraction (E–C) coupling, but many reports do not support the idea that the increase in $[Ca^{2+}]_i$ through E–C coupling between L-type Ca^{2+} channel and ryanodine receptor is coupled to NFAT activation (Wilkins and Molkentin, 2004).

A possible source of Ca^{2+} for activation of calcineurin is Ca^{2+} influx through transient receptor potential (TRP) proteins that are involved in store-operated Ca^{2+} entry (Clapham, 2003). Upregulation of canonical transient receptor potential (TRPC) proteins is recently reported to contribute to

*Corresponding author. Department of Pharmacology and Toxicology, Graduate School of Pharmaceutical Sciences, Kyushu University, 3-1-1 Maidashi, Higashi-ku, Fukuoka 812-8582, Japan.
Tel./Fax: +81 92 642 6884; E-mail: kurose@phar.kyushu-u.ac.jp

Received: 10 February 2006; accepted: 11 October 2006; published online: 2 November 2006